Clustering-Based Analysis of Green Area Reduction and Thermal Impact in Marabá-PA

Mayara Ferreira[1], **Vitor Castro**[1], **Marcela Alves**[1], **Hugo Kuribayashi**[1]

[1]ManivaLab - Grupo de Pesquisa em Transformação Digital na Amazônia Sul Oriental
Universidade Federal do Sul e Sudeste do Pará (Unifesspa) - Marabá, PA - Brasil

{mayaralves, vitor, marcela.alves, hugo}@unifesspa.edu.br

Abstract. *This study investigates the thermal impact related with the reduction of green areas in the municipality of Marabá-PA through the analysis of satellite imagery and the application of Machine Learning (ML) clustering techniques. The temporal evaluation reveals a significant expansion of urban areas accompanied by a marked decline in vegetated regions. The results demonstrate a strong correlation between decreased green cover and increased land surface temperatures, exacerbating the effects of the local heat island. These findings underscore the urgent need for integrated environmental preservation strategies and the implementation of public policies that promote sustainable urban growth. Recommendations include prioritizing the restoration of green infrastructure, adopting integrated urban planning that respects historical land use patterns, and balancing economic development with the conservation of natural resources to mitigate thermal impacts and improve regional quality of life.*

1. Introduction

In recent years, the rise in global temperature has become increasingly evident, with annual data revealing a consistent upward trend. According to the Copernicus Climate Change Service (C3S) report, the average global temperature in 2024 reached 1.5°C above the pre-industrial period (1850–1900) [Copernicus Climate Change Service 2025]. Furthermore, data from the National Institute of Meteorology (INMET) indicate that 2024 was the hottest year in Brazil since 1961, with an average temperature 0.79°C higher than the historical mean [INMET 2025].

This marked increase in temperature has been linked to various human activities in recent decades that have progressively intensified the effects of climate change. Among the main factors are deforestation, wildfires, accelerated urbanization, and the growth of greenhouse gas emissions. Although these activities occur around the world, they have a more pronounced impact in sensitive areas such as the Amazon region. The Amazon contains the largest tropical forest on Earth and plays a critical role in the carbon cycle and global climate regulation. Therefore, it is considered a high-risk region with respect to climatic influences [Zogahib et al. 2024].

One perspective on climatic variations in the Amazon refers to the relationship between these changes and deforestation for the expansion of agricultural systems. This process results in the transfer of carbon from the biosphere to the atmosphere in the form of carbon dioxide, thereby intensifying these climatic alterations. Deforestation is also associated with a reduction in air humidity, as the absence of vegetation decreases evapotranspiration, exacerbating the hot and dry climate in the Amazon [Nobre et al. 2007].

In contrast, extreme heat constitutes a serious public health concern. According to the related literature, prolonged exposure to high temperatures increases the incidence of diseases (morbidity) and contributes to elevated mortality rates, disproportionately affecting the elderly, children and individuals with pre-existing health conditions, which can lead to death in severe cases [Faurie et al. 2022, Song et al. 2021, Mandú et al. 2021]. Furthermore, heat stress also adversely affects mental health, decreases physical work capacity, and alters cognitive performance [Cheveldayoff et al. 2023, Ebi et al. 2021].

In this context, the relationship between changes in green areas and local climate variations becomes a pertinent topic for understanding environmental and climatic impacts, making the formulation of mitigation strategies essential. Vegetation cover plays a fundamental role in the regulation of the microclimate, influencing temperature, humidity, and air quality, especially in regions characterized by intense urban occupation and agricultural expansion [Sheng et al. 2025, Wang et al. 2022].

Furthermore, the related literature highlights several studies, such as [De Andrade et al. 2023, Kalnay and Cai 2003], which have investigated the relationship between anthropogenic alterations and increasing temperatures. However, a significant portion of these analyses focus primarily on the influence of urbanization on local climate, while the direct association between warming and the reduction of green areas in other contexts remains underexplored. In addition, most studies employ conventional approaches that may be limited in capturing the temporal and spatial complexity of the areas studied over time. Hence, how to effectively model and monitor the nuanced, multiscale changes in green cover and their thermal impacts represents a significant challenge. In this regard, the integration of Machine Learning (ML) techniques presents promising opportunities to enhance the identification and monitoring of these variations, allowing more precise and dynamic analyzes.

Thus, this study conducts an evaluation of the temporal variation of green areas and the associated Land Surface Temperature (LST) impact on climatic changes in municipalities within the Amazon region, focusing on the municipality of Marabá-PA as a case study. The research involves the processing and analysis of satellite imagery to assess the municipality's temperature, in addition to applying unsupervised learning methods through clustering on the Google Earth Engine (GEE) platform to classify land use.

The remainder of this work is organized as follows: Section 2 reviews related work, while Section 3 details materials and methods used. Furthermore, Section 4 discusses the results, and Section 5 concludes the paper with key findings.

2. Related Work

The related literature includes numerous studies aimed at understanding the dynamics between deforestation and climatic variations to support the development of mitigation strategies for this complex issue that impacts the planet as a whole.

In [De Andrade et al. 2024], the authors investigate local climate changes in two Brazilian cities, Cajazeiras-PB and São Félix do Xingu-PA, analyzing the relationship between land use and temperature variations from 1990 to 2022. Using statistical models such as AutoRegressive Moving Average with eXogenous inputs (ARMAX) and ML, the study quantifies the impact of urban, agricultural and forested areas on temperatures,

utilizing data from INMET and MapBiomas[1]. The results highlight the influence of urban and agricultural zones on the increase in local temperatures, emphasizing the significance of land use in climatic changes. However, the methodology adopted may face challenges related to the availability of meteorological data from INMET, as inadequate maintenance of weather stations can compromise data quality and continuity. For example, in the municipality of Marabá-PA, INMET data have been unavailable since 2017, hindering access to reliable local meteorological information necessary for detailed analyses.

The studies by [da Silva et al. 2021] and [da Silva et al. 2022] analyze the impact and consequences of accelerated urban development in Marabá-PA and Curitiba-PR cities over the past 30 years. Both investigations used satellite imagery from *Landsat* 5 and 8, combined with land use and occupation data from the MapBiomas platform, to capture surface temperature information. In Marabá, the results indicate a reduction of 43.86% in the vegetated area, accompanied by a 35.26% increase in maximum temperatures, thus intensifying the heat islands in the city. Similarly, in Curitiba, urban expansion promoted the formation of heat islands, whereas the presence of green areas contributed to the appearance of small cold islands. However, the approach focuses exclusively on urban areas, disregarding the influence of the rural area, which also affects the regional microclimate. Furthermore, the use of MapBiomas to analyze the most recent years may represent a limitation, since the platform requires a time lag to provide annual updates.

In [da Silva Santos et al. 2021], the authors investigate the climate change in the municipality of Alta Floresta-MT and its relationship with the change in land use. Data were obtained from multiple sources, with particular emphasis on ERA-IECMWF. To identify correlations and trends between climatic variables and environmental indicators, the study employs statistical techniques such as linear regression and regression through change point analysis. The results indicate that deforestation and wildfires have contributed significantly to climatic changes in the region, leading to increased temperatures and decreased air humidity. However, the choice of ERA-IECMWF as the temperature data source presents a limitation, as its low spatial resolution does not permit detailed local analyses, potentially compromising the accuracy of the findings.

The studies analyzed demonstrate, through various methodologies, the dynamic relationship between changes in land use and climatic variations, emphasizing the influence of deforestation and rapid urbanization on the increase in local temperatures. Thus, our approach differs from that of other studies in the following ways:

- This study employs unsupervised clustering algorithms, notably K-means and Cascade K-means, implemented through the GEE platform, to classify and monitor changes in land cover during the period analyzed (2014-2024). In contrast, related studies predominantly utilize traditional statistical models, focusing on the analysis of climatic and environmental variables using tabular data;
- This work performs a detailed spatial analysis of LST associated with land use changes using Landsat satellite imagery and MapBiomas data, enabling identification of local warming patterns linked to urbanization and vegetation loss. Related studies often use meteorological stations or climate reanalysis data with coarser spatial resolution, limiting precision in local microclimate assessment;

[1]Available at: https://brasil.mapbiomas.org

- Finally, while related works investigate climate change and its relationship with environmental variables in diverse regional contexts, this study aims to link temporal changes in vegetation cover identified through satellite-based classification with thermal dynamics in the Amazonian municipality of Marabá-PA, thereby providing practical contributions toward local environmental mitigation policies.

3. Experimental Design and Materials

This section provides an overview of the municipality of Marabá-PA, encompassing its geographical and socioeconomic characteristics, as well as the approaches and techniques employed for the temporal analysis of the change in vegetation cover in the region and its association with climatic variations. ML techniques, particularly clustering tasks, are adopted and elaborated herein with the objective of classifying and monitoring changes in land use cover over time. Furthermore, this section details the data sources utilized and the corresponding data processing procedures.

3.1. Overview of Marabá: Geography, Population and Economy

The municipality of Marabá, located in the southeast of the state of Pará, is the focus of this study. Covering an area of 15,127.872 km², with 62.49 km² urbanized as of 2022, Marabá has a population of 266,533 inhabitants, ranking fifth among the most populous cities in the state of Pará. In 2021, its Gross Domestic Product (GDP) per capita was recorded at R$ 47,010.21 by the Brazilian Institute of Geography and Statistics (IBGE), while its most recent municipal Human Development Index (HDI), registered in 2010, was 0.668. Furthermore, the primary economic activities of Marabá currently lie within the agriculture and livestock, industrial, and service sectors [IBGE 2022].

Located in the Amazon region, the climate is characterized by two distinct periods: the rainy season, spanning from November to March, and the dry season, prevailing from May to September [Fisch et al. 1996]. During the dry season, elevated temperatures and reduced humidity create favorable conditions for increased occurrences of wildfires and deforestation in the area, which release toxic particles and gases resulting from vegetation burning, thus exacerbating impacts on public health and the environment.

3.2. Data Acquisition and Transformation

For the analysis of LST, this study uses satellite data provided by the United States Geological Survey (USGS). The selected dataset corresponds to the Landsat 8-9 Operational Land Imager (OLI)/Thermal Infra-Red Sensor (TIRS) Collection 2 Level 2, specifically band 10, which has a spatial resolution of 30 meters and is employed to estimate the Earth's surface temperature. To ensure data quality, images with zero cloud cover (0%) were filtered for the period 2014 to 2024, resulting in the selection of images from June to August, which correspond to the warmest period in the municipality.

The temperature calculation (T) adhered to the specifications outlined in the dataset documentation [USGS 2023] (Equation 1). A scale factor of 0.00341802 and an additive offset of 149 were applied to band 10 of the TIRS. These parameters enable the conversion of the satellite's raw data to Kelvin units. Subsequently, subtracting 273.15 converts the values to the Celsius scale. This methodology allows for the estimation of thermal variation within the municipality during the warmest months, as follows:

$$T = (\text{Band } 10 \times 0.00341802) + 149 - 273.15. \quad (1)$$

Within the GEE, the *Landsat* 8 *Collection* 2 Level 2 Tier 1 dataset was used, whose images possess a spatial resolution of 30 meters. A filter was applied to exclude images with cloud cover exceeding 1%, minimizing their influence on the results. A False Color band combination was selected for the analysis of the area of interest, using bands 7 (Shortwave Infrared 2), 6 (Shortwave Infrared 1), and 4 (Red) of the collection. The analyzes were conducted over the period 2014 to 2024. Following filter application, the images were normalized and 1,500 random points were sampled for the clustering process. In addition, the platform was used to calculate the areas of the resulting clusters to support the analysis of the study.

Furthermore, this study also employs the detection of a change point within a time series of annual mean temperatures, using a simplified version of the Pettitt statistical test. This nonparametric test is utilized to identify abrupt shifts in the median of the series, indicating a potential structural break or regime change in the data over time. Following the identification of this breakpoint, the series u is constructed, representing the segmented means of the original series before and after the change point, thus enabling a clear visualization of the two distinct phases within the temporal series. This segmentation facilitates the analysis of climatic variation and improves the understanding of impacts associated with environmental changes and changes in land cover in the studied region.

3.3. Clustering Methods

The clustering was performed using GEE, which also provides advanced geospatial analysis tools. GEE offers a variety of supervised and unsupervised ML methods for image classification. The algorithms selected for the clustering task were *K-means* and *Cascade K-means*, chosen due to their widespread use and low computational complexity.

For clustering, the methodology adopted in this study refers to the land cover classes defined by the MapBiomas project [MapBiomas 2024]. Consequently, five main classes are considered: **Forest** (dense concentration of vegetation), **Herbaceous Vegetation** (non-woody plants such as herbs and grasses), **Agricultural Areas** (Farming and livestock), **Non-Vegetated Areas** (urban areas, beaches, mining areas and other surfaces lacking significant vegetation) and **Water bodies** (rivers, wetlands, and reservoirs).

Among the ML algorithms employed in this study, the *K-means* method is an unsupervised learning technique aimed at partitioning the dataset into k subsets, based on data similarity [Arthur and Vassilvitskii 2007, Calinski and Harabasz 1974]. Partitioning is performed through distance calculations. Initially, random points are selected as cluster centers and the remaining points are assigned to the nearest centers. Subsequently, these centers were recalculated to represent the mean of all the elements assigned to each cluster. This process of point reassignment and centroid updating iterates until there is no significant change in the centers, indicating stabilization of the clusters. The algorithm seeks to minimize the sum of squared errors (E) as follows:

$$E = \sum_{i=1}^{k} \sum_{x \in C_i} ||x - x_i||^2, \quad (2)$$

where k denotes the hyperparameter corresponding to the number of clusters, C_i represents the set of points assigned to the i-th cluster and x_i denotes the centroid of the cluster C_i. In addition, $||x - x_i||$ represents the distance between an individual point x and the centroid x_i. The function defined by Equation 2 quantifies the total clustering error, with the aim of the algorithm being to minimize the value of E. Consequently, the smaller the value of E, the greater the intra-cluster similarity of the formed clusters.

Conversely, the *Cascade K-means* algorithm aims to optimize the traditional *K-means* methodology, particularly when dealing with large volumes of data. It partitions the data into smaller subgroups and applies the *K-means* algorithm to each subgroup. Subsequently, the results are adjusted and reallocated to a reduced number of clusters until the desired number k of clusters is attained. This process is iterative and terminates when no significant changes occur or when the predefined stopping criterion is met.

Within the context of the *Cascade K-Means* algorithm, the distance between points within the clusters was calculated using the Euclidean metric $d(x_i, y_j)$, as defined in Equation 3. This metric is widely used in this method, as it enables an efficient assessment of similarity between points at each stage of the cascading process, thereby contributing to a more refined and hierarchical segmentation of the data, as follows:

$$d(x_i, y_j) = \sum_{i=1}^{n} (x_i - y_j)^2, \tag{3}$$

where x_i and y_j denote the coordinates of the points in the attribute space, such that x_i belongs to a specific cluster and y_j serves as a reference point (e.g., a centroid or another point of comparison); n represents the dimensionality of the data, and the summation computes the squared Euclidean distance between the points.

3.4. Evaluation Metric

The silhouette index (S_i) was used as an evaluation metric to assess the quality of the groupings obtained. In this validation method, for each point, the average distance between that point and all other points within the same cluster is calculated. Subsequently, the average distance between the point and all points in the nearest-neighboring cluster is determined [Rousseeuw 1987]. Based on these assumptions, S_i is computed as follows:

$$S_i = \frac{b_i - a_i}{\max(a_i, b_i)}, \tag{4}$$

where a_i denotes the average distance between point i and the other points within its own cluster, while b_i represents the average distance between point i and the points in the nearest neighboring cluster to which it does not belong. The results of this metric lie within the interval $[-1, 1]$, where values closer to 1 indicate well-clustered groups, while values closer to -1 imply that the clusters may be misclassified.

4. Results and Discussion

The experiments were carried out by setting the hyperparameter $k = 5$, corresponding to the number of classes defined for the classification of land use. Furthermore, the exper-

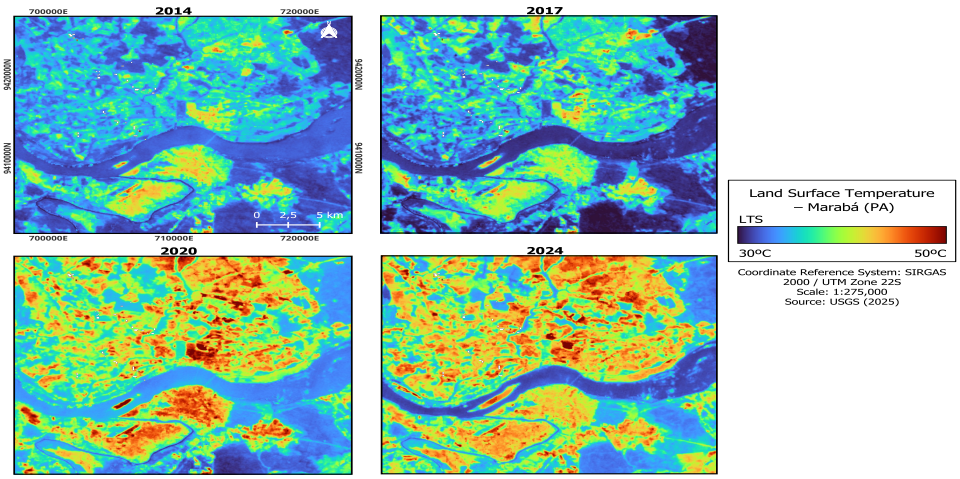

Figure 1. Surface Temperature Map of the City of Marabá.

iments were implemented using the JavaScript programming language via GEE, which facilitates the application of ML algorithms and the analysis of geospatial data.

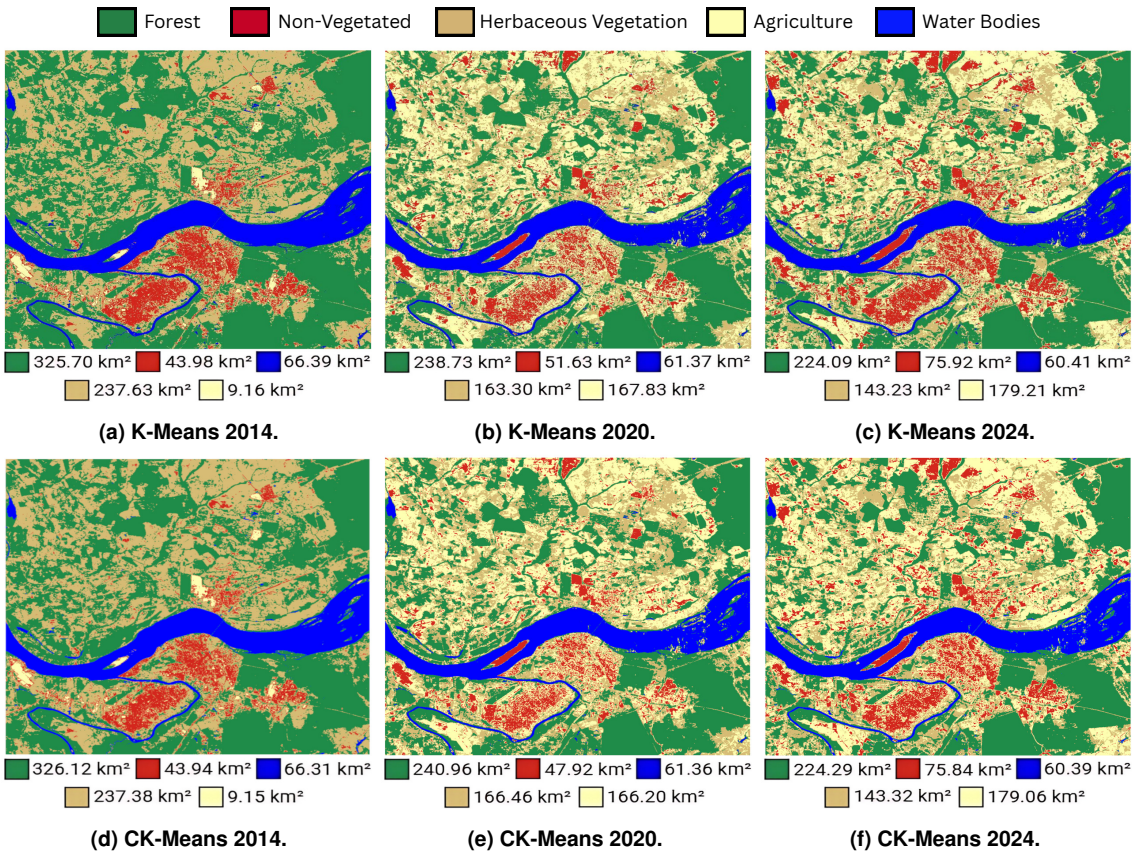

(a) K-Means 2014. **(b) K-Means 2020.** **(c) K-Means 2024.**

(d) CK-Means 2014. **(e) CK-Means 2020.** **(f) CK-Means 2024.**

Figure 2. Land use maps of the Marabá region during the 2014-2024 period.

Figure 1 depicts a LST map of the municipality of Marabá-PA for the period 2014-2024. The color scale ranges from blue (30°C) to red (50°C), indicating that cooler areas, such as bodies of water and dense vegetation, have been replaced by warmer regions associated with urbanization and deforestation. In 2014, blue, green, and yellow hues pre-

dominated, with higher temperatures concentrated primarily in urban areas, while forested regions maintained milder temperatures. In 2017, an increase in yellow and orange areas emerged, signifying progressive warming. In 2020, a significant expansion of the red zones was observed, indicating that increases in temperature had begun to extend beyond urban limits. By 2024, the predominance of red tones suggests a substantial rise in surface temperature, linked to vegetation reduction and intensified urbanization.

Figure 2 presents the land use and land cover maps obtained by clustering using the K-means and Cascade K-means algorithms, respectively. The values used to analyze vegetation variation were derived from the average of the results generated by both clustering methods. In 2014, the forest areas (green) identified by the clusters exhibited an average of 325.90 km2, while herbaceous vegetation (brown) and non-vegetated areas (red) totaled, respectively, 237.50 and 53.10 km^2. In 2017, changes in land cover were observed: the average forest area decreased by approximately 29.77%, reaching 278.06 km^2. Herbaceous vegetation decreased by 9.44%, totaling 215.08 km^2. In contrast, non-vegetated areas increased by 24.61%, attaining an average of 66.17 km^2.

However, the results obtained indicate a trend of reduction in native vegetation. During this period, forest areas and herbaceous vegetation areas experienced approximate decreases of 31.2% and 32.1%, respectively. In contrast, non-vegetated areas underwent an expansion of 42.9% over the period, which is associated with the increase in urban areas and deforestation in the region. In this context, the agriculture and livestock area registered an increase of 20.8% in the analyzed period.

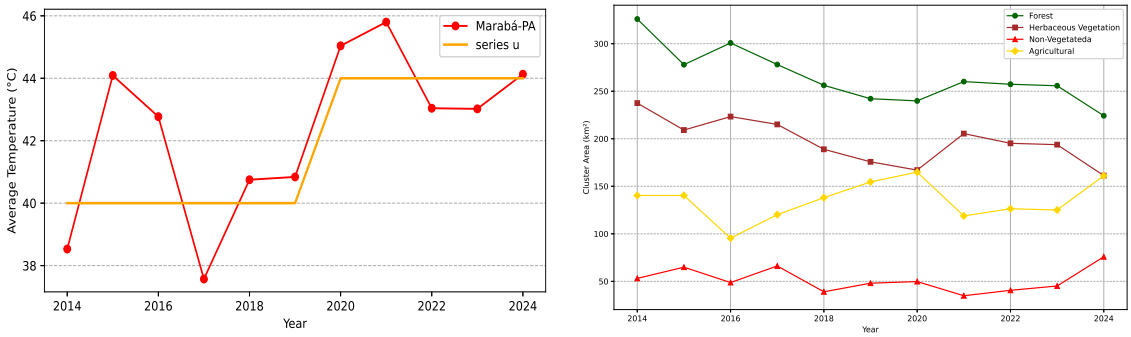

(a) Evolution of the recorded average temperature in Marabá-PA (2014-2024).

(b) Evolution of land use in Marabá-PA (2014-2024).

Figure 3. Evolution of land use and average temperature in Marabá-PA (2014–2024), highlighting land cover changes and temperature rise.

Figure 3 summarizes the evolution of land use and the average temperature in Marabá-PA during the analyzed period, highlighting changes in land cover and the rise of temperatures. In particular, Figure 3a displays the temperature series together with Pettitt's u depicted throughout the series, highlighting the identified change point. Between 2014 and 2016, there is a sharp increase in temperature followed by a decline, while between 2016 and 2020, high volatility is observed, possibly due to seasonal fluctuations or extreme events such as droughts and heatwaves. After 2020, the temperature continues to fluctuate but exhibits an upward trend, as indicated by the change point detected by the series u, reaching elevated values in 2024. In general, the temperature shows an increasing trend, increasing from 38.52°C in 2014 to 44.12°C in 2024, corresponding to

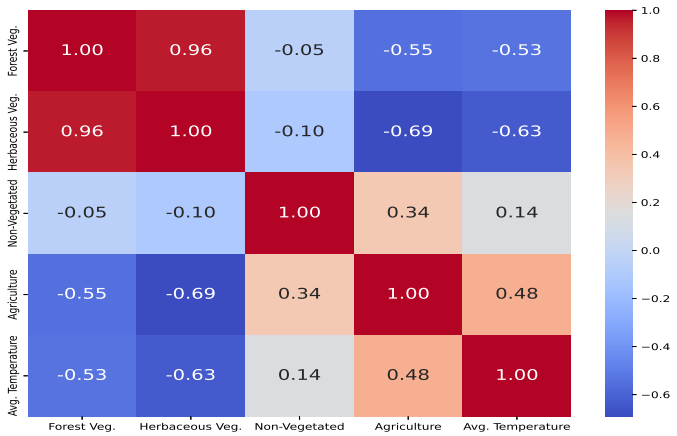

Figure 4. Correlation map of land use cover areas.

a variation of 5.60°C over the decade.

Furthermore, Figure 3b highlights changes in land cover, suggesting a pattern of environmental transformation. Vegetated areas exhibit a declining trend attributed to deforestation and conversion to other land uses. Thus, the observed spatial organization not only reflects a historical pattern that exacerbates adverse patterns of land use and occupation, thus increasing environmental and social degradation. The Non-Vegetated coverage fluctuates over the years, indicating dynamic changes in land use, such as environmental degradation or unplanned urbanization. Moreover, the area allocated to *Agriculture* exhibits continuous growth in recent years, suggesting an expansion of agricultural activity, thus revealing land occupation patterns that are influenced by the economic and social agents operating in the region.

Furthermore, Figure 4 presents a correlation map between variables of land use cover types over the period considered. The map highlights a strong positive correlation between the vegetated areas, as well as a negative correlation between these and the agricultural areas, indicating a competition between the preservation of green spaces and the expansion of one of the main economic activities of the region (farming and livestock). Furthermore, the average temperature of the region exhibits a negative correlation with the vegetated areas, suggesting that as these areas decrease, the mean temperature tends to increase. This relationship implies that the loss of vegetation cover contributes to the warming of the local microclimate due to the reduced evapotranspiration and the altered thermal properties of the soil.

In addition, the silhouette index was used to assess the quality of the generated clusters by measuring both the internal cohesion and the separation between clusters. Table 1 indicates values ranging from 0.52 to 0.59, demonstrating a good consistency in the formation of the clusters. However, a slight downward trend in the values is observed, which is related to changes in land use patterns or increased difficulty in distinguishing between classes with similar spectral characteristics. It is noted that, in 2014, the cluster associated with agricultural areas had a less prominent representation in the groupings compared to the following years. Over the analyzed period, this cluster became more expressive in the segmentation, increasing the complexity of the images. The relative increase in the presence of this group, combined with the growing visual complexity of

the images, contributed to the slight reduction in the calculated silhouette index.

Table 1. Silhouette Coefficient Values for Cluster Model Validation.

Year	Cascade K-means	K-means
2014	0.5976	0.5977
2017	0.5721	0.5835
2020	0.5554	0.5513
2024	0.5290	0.5271

The results indicate that land use patterns have influenced micro-climatic changes in the region. In this context, Figure 5 aims to map this correlation dynamic, highlighting four categories: areas without change and without increase in temperature (blue), without change but with an increase in temperature (gray), with change but without an increase in temperature (green) and with both change and increase in temperature (red). To generate this map, the GEE was initially used to create a binary image indicating areas where changes in land use occurred over time. The subtraction between the heat maps from 2014 to 2024 allowed the identification of areas with thermal variation (increase of 5°C). Finally, the subtraction between the binary maps of land use and the temperature variation was performed, resulting in the final map that enables the spatial visualization of the correlation between the change in land use and the increase in temperature. Hence, this approach reinforces the findings derived from the clustering analysis, demonstrating a consistent correlation between land use changes and temperature variations.

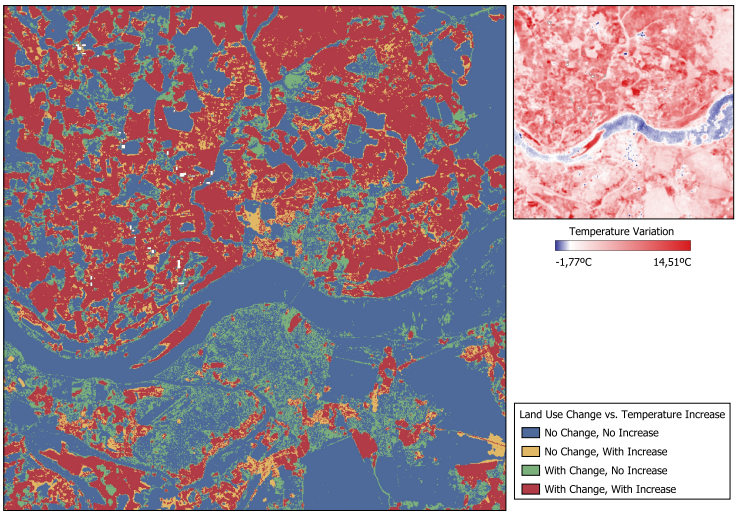

Figure 5. Land Cover Change and Temperature Increase.

Areas undergoing significant changes in land cover are observed to exhibit a marked increase in temperature, suggesting that anthropogenic activities, such as deforestation and urbanization, are directly associated with local warming. In contrast, regions where land cover remained unchanged tend to maintain more stable temperatures, indicating that the preservation of vegetation cover may contribute to mitigating the effects of heat island. Thus, the map underscores the importance of sustainable territorial planning to reduce negative climatic impacts.

In this context, accelerated urbanization, coupled with the lack of effective planning policies, reinforces land use patterns that intensify alterations in the region's microclimate. Urban expansion and intensified land use underscore the urgent need to integrate strategies that promote urban sustainability, including the restoration of degraded areas, prioritization of green infrastructure, and integrated urban planning that acknowledges the region's historical patterns and economic dynamics.

5. Conclusions and Implications

The results of this study indicate a significant increase in temperatures over the years, with elevations in both minimum and maximum temperatures in the analyzed region. Concurrently, there is an observed reduction in forest and herbaceous vegetation areas, accompanied by the expansion of non-vegetated areas. This suggests a notable influence of vegetation loss on the thermal impact experienced in the region. The findings reveal a correlation between changes in land cover and temperature variations, as regions where temperatures increased beyond urban areas coincide with those most affected by vegetation reduction and the expansion of non-vegetated zones.

The adopted methodology study demonstrated promising performance in identifying land cover patterns, enabling the establishment of a relationship between its variation and the increase in temperatures. Future research should incorporate additional meteorological variables, in order to enrich the investigation and provide a clearer understanding of thermal variations. Finally, this study underscores the need for public policies focused on mitigating environmental impacts caused by anthropogenic changes, which can contribute to reducing thermal impact and improving the quality of life for the region's population. Such policies must recognize the historical patterns of the region, balancing urban and economic growth, natural resource preservation, and collective well-being.

References

Arthur, D. and Vassilvitskii, S. (2007). K-means++: The Advantages of Careful Seeding. In *Proceedings of the Eighteenth Annual ACM-SIAM Symposium on Discrete Algorithms*, pages 1027–1035.

Calinski, T. and Harabasz, J. (1974). A Dendrite Method for Cluster Analysis. *Communications in Statistics*, 3:1–27.

Cheveldayoff, P. et al. (2023). Considerations for occupational heat exposure: A scoping review. *PLOS Climate*, 2(9):1–21.

Copernicus Climate Change Service (2025). Global Climate Highlights 2024.

da Silva, J. C. R. et al. (2022). Sensoriamento Remoto para Análise de Ilhas de Calor e Frio no Município de Curitiba: Remote sensing for heat and cold island analysis in the city of Curitiba. *Studies in Environmental and Animal Sciences*, 3(2):406–415.

da Silva, J. P. S., Loureiro, G. E., and de Sousa, I. (2021). Análise Espaço-Temporal da Temperatura da Superfície Terrestre na Cidade de Marabá, Pará, Brasil. *Research, Society and Development*, 10(7):e41710716718–e41710716718.

da Silva Santos, K., Oliveira, B. F. A., and Ignotti, E. (2021). Mudanças Climáticas e suas Relações com o Uso da Terra no Município de Alta Floresta-Amazônia Meridional Brasileira. *Biodiversidade Brasileira*, 11(3).

De Andrade, J. V. et al. (2024). Exploring Climatic Shifts in Brazilian Climates: Insights from ARMAX, Decision Trees, and Artificial Neural Networks. In *Brazilian Conference on Intelligent Systems*, pages 167–179. Springer.

De Andrade, J. V. R. et al. (2023). Assessing the Effect of Urban Expansion and Deforestation on Temperature Rise in Cajazeiras, Brazil: A Data-Driven Approach. In *2023 IEEE Latin American Conference on Computational Intelligence (LA-CCI)*, pages 1–6.

Ebi, K. L. et al. (2021). Hot Weather and Heat Extremes: Health Risks. *The lancet*, 398(10301):698–708.

Faurie, C. et al. (2022). Association between high temperature and heatwaves with heat-related illnesses: A systematic review and meta-analysis. *Science of The Total Environment*, 852:158332.

Fisch, G., Marengo, J. A., and Nobre, C. A. (1996). Clima da Amazonia. *Climanálise - Boletim de Monitoramento e Análise Climática*, x:24–41.

IBGE (2022). Panorama do Município de Marabá - PA. Disponível em: `https://cidades.ibge.gov.br/brasil/pa/maraba/panorama`.

INMET (2025). 2024 foi o Ano mais Quente no Brasil desde 1961. Disponível em: `https://portal.inmet.gov.br/noticias/2024--o-ano-mais-quente-da-srie-histrica-no-brasil`.

Kalnay, E. and Cai, M. (2003). Impact of Urbanization and Land-use Change on Climate. *Nature*, 423(6939):528–531.

Mandú, T. B. et al. (2021). Impacto das Ondas de Calor no Conforto Térmico Humano na Região da Floresta Nacional do Tapajós, Oeste do Pará. *Biodiversidade Brasileira*, 11(4):98–108.

MapBiomas (2024). Códigos de legenda. Disponível em: `https://brasil.mapbiomas.org/codigos-de-legenda/`.

Nobre, C. A., Sampaio, G., and Salazar, L. (2007). Mudanças climáticas e Amazônia. *Ciência e Cultura*, 59(3):22–27.

Rousseeuw, P. J. (1987). Silhouettes: a graphical aid to the interpretation and validation of cluster analysis. *Journal of computational and applied mathematics*, 20:53–65.

Sheng, Q. et al. (2025). The mediating effect of microclimate in the impacts of roadside vegetation barriers on air pollution in pedestrian spaces. *Building and Environment*, 279:113052.

Song, J. et al. (2021). Ambient high temperature exposure and global disease burden during 1990–2019: An analysis of the global burden of disease study 2019. *Science of The Total Environment*, 787:147540.

USGS (2023). Landsat 8-9 Coll. 2 L2 Science Product Guide.

Wang, C. et al. (2022). Effects of vegetation restoration on local microclimate on the loess plateau. *Journal of Geographical Sciences*, 32(2):291–316.

Zogahib, A. L. N. et al. (2024). Climate Xhanges and Its Impacts on Cities: Case Study of Characteristics of The Drought in The State of Amazonas, Brazil. *Research, Society and Development*, 13(9):e9913946940.